

Spatial and temporal modeling of wetland surface temperature using Landsat-8 imageries in Sulduz, Iran

Vahid Eisavi^{*1}, Ahmad Maleknezhad Yazdi², Seyed Ali Niknezhad³

¹Tarbiat Modares University, Remote Sensing and GIS Department, M.Sc. in Remote Sensing, Tehran, Iran

²University of Tehran, Natural Resources, M.Sc. in Combating Desertification Department, Tehran, Iran

* Corresponding author e-mail (İletişim yazarı e-posta): esavi.vahid@gmail.com

Received (Geliş tarihi): 25.12.2014 - Revised (Düzelme tarihi): 24.01.2015 - Accepted (Kabul tarihi): 24.01.2015

Abstract: Wetland Surface Temperature (WST) maps are an increasingly important parameter to understand the extensive range of existing processes in wetlands. The Wetlands placed in neighborhoods of agricultural and industrial lands are exposed to more chemical pollutants and pesticides that can lead to spatial and temporal variations of their surface temperature. Therefore, more studies are required for temperature modeling and the management and conservation of these variations in their ecosystem. Landsat 8 time series data of Sulduz region, Western Azerbaijan province, Iran were used in this study. The WST was derived using a mono-window algorithm after implementation of atmospheric correction. The NDVI (Normalized Differential Vegetation Index) threshold method was also employed to determine the surface emissivity (ϵ_λ). Our findings show that the WST experienced extensive spatial and temporal variations. It reached its maximum value in June and also experienced the highest mean in the same month. In this research, August (12.08.2013) had a lowest spatial standard deviation regarding surface temperature and June (28.06.2013) had the highest one. Wetlands' watersides adjacent to industrial zones have a higher surface temperature than the middle lands of these places. The map obtained from the WST variance over time can be exploited to reveal thermal stable and unstable zones. The outcome demonstrates that land use, land cover effectively contribute to wetland ecosystem health. The results are useful in the water management, preventive efforts against drying of wetland and evapotranspiration modeling. The approach employed in this research indicates that remote sensing is a valuable, low-cost and stable tool for thermal monitoring of wetlands health.

Keywords: WST, spatial variations, temporal variations, NDVI

İran Sulduz bölgesinde Landsat-8 uydu görüntüleri kullanılarak sulak alanların yüzey sıcaklığının mekansal ve zamansal olarak modellenmesi

Özet: Sulak alanların yüzey sıcaklık (WST) haritaları, sulak alanlarda mevcut süreçlerin geniş kapsamlı olarak anlaşılmasında giderek daha önemli bir parametre haline gelmektedir. Tarım ve sanayi arazilerine komşu sulak alanlar, daha fazla kimyasal kirlenici ve pestisit maruz kalması nedeniyle, yüzey sıcaklığının mekansal ve zamansal değişimlere neden olabilmektedir. Bu nedenle, sıcaklık modellemesi ve zamansal ve mekansal değişimlerin tespit edilmesi, sulak alan ekosistemlerinde korunması ve yönetimi için daha fazla çalışma gereklidir. Bu çalışmada, İran Sulduz bölgesine ait Landsat 8 zaman serisi verileri kullanılmıştır. WST haritaları atmosferik düzeltmeler yapıldıktan sonra tek pencere (mono-window) algoritmaları kullanılarak türetilmektedir. Ayrıca Normalleştirilmiş Fark Vejetasyon İndeksi (NDVI) (Normalized Differential Vegetation Index)'de yüzey emisyonunu belirlemede kullanılmaktadır. Bulgularımız WST haritalarının geniş zamansal ve mekansal varyasyonlar içerdiğini göstermiştir. En yüksek değer ve en yüksek ortalama Haziran ayında olmaktadır. Araştırmada yüzey ısısı açısından Ağustos ayı (12.08.2013) en düşük mekansal standart sapmayı gösterirken, en yüksek mekansal standart sapma değeri ise Haziran ayı (28.06.2013)'nda olmuştur. Endüstriyel alanlara bitişik sulak alanlar daha iç kısımlardakilere nazaran daha yüksek yüzey ısısına sahiptirler. WST'lerden elde edilen haritalar ısısal olarak stabil ve stabil olmayan alanların belirlenmesinde kullanılabilir. Sonuçlar; arazi kullanımı ve arazi örtüsünün sulak alanlar ekosisteminin sağlık durumunu etkilediğini göstermektedir. Bu açıdan elde edilen sonuçlar, su yönetimi, sulak alanların kurumaması için alınabilecek önlemlere ve evapotranspirasyon modellemesine katkıda bulunacaktır. Bu çalışmadaki yaklaşım; uzaktan algılamanın değerli, düşük maliyetli ve sulak alanların sıcaklık değerlerinin izlenmesi açısından son derece uygun bir araç olduğunu göstermektedir.

Anahtar Kelimeler: WST, mekansal değişkenler, zamansal değişkenler, NDVI

To cite this article (Atıf): Eisavi, V., Maleknezhad, Y., Niknezhad, S.A., 2016. Spatial and temporal modeling of wetland surface temperature using Landsat-8 imageries in Sulduz, Iran. *Journal of the Faculty of Forestry Istanbul University* 66(1): 46-58. DOI: [10.17099/jffiu.26733](http://dx.doi.org/10.17099/jffiu.26733)



1. INTRODUCTION

Wetland Surface Temperature (WST) maps are an increasingly important parameter to understand the extensive range of existing processes such as follows: evaporation and surface water transfer patterns (Strub and Powell, 1986; Strub and Powell, 1987; Steissberg et al., 2005; Oesch et al., 2008), Monitoring water quality (Reinart and Reinhold, 2008; Coats 2010), Phytoplankton dynamics and primary production (Wooster et al., 2001; Thiemann and Schiller 2003), Oxygen concentration in water (Matzinger et al., 2007), and the denitrification rate (Bremner and Shaw 1958; Beauchamp et al., 1989). Warming of wetlands leads to the water thermal stability and resistance to mixing, which on one hand may increase growth of harmful algae (Paerl and Paul 2012), and on the other hand, affects aquatic animals' colonies (Jeppesen et al., 2012). Further, the wetlands where located adjacent of agricultural lands receive heavy sediment loads (Piano and Wang 2011), chemical fertilizers and pesticide (Klotz 1985; Sharpley and Withers 1994; Harding et al., 1999; Gleason et al., 2003; Relyea 2005). A large influx of these harmful materials results in spatial and temporal variations of the WST, which affects these ecosystems substantially (Mortsch and Quinn 1996; Bergstedt et al., 2003; Cooke et al., 2004; Gillet and Péquin 2006; Ham et al., 2006).

Effective wetlands management requires thorough understanding of ecosystem components and the way in which they interact (Gilman 1994). Accordingly, wetlands temperature is an influential and principal component on the environment. Although, estimation of this parameter by traditional methods like ground sampling and interpolation is a costly and time-consuming procedure, remote sensing is a powerful tool for studying environment which can provide systematic and periodic coverage of the inaccessible regions (Dash et al., 2002; Novo et al., 2006; Alcantara et al., 2009). Moreover, remote sensing obtains information in digital format which can be easily integrated with the other geographic information or merely utilized for quantitative modeling (Lamaro et al., 2013). Studies were performed regarding the application of remote sensing and satellite imagery in the calculation of the WST (Mustard et al., 1999; Cherkauer et al., 2005; Zoran et al., 2005; Ahn et al., 2006; Alcantara et al., 2010; Gibbons and Wukelic 1989), in which researchers employed different sensors such as AASTR (Schneider et al., 2009), MODIS (Wan 2008; Chavula et al., 2009), AVHRR (Bussi eres and Granger 2007), Landsat (Oesch et al., 2008) ASTER (Steissberg et al., 2005) and SEVIRI (Nehorai et al., 2009) to estimate this parameter. To recapitulate these studies, we can state that more researches are required for spatial-temporal variation modeling of WST which facilitates the management and conservation of these ecosystems.

2. MATERIALS AND METHODS

2.1 Study Area

The study area is Sulduz region at an elevation of 1,300 meters above sea-level, located in West Azerbaijan Province, northwest of Iran (Figure /  ekil 1). The climate of the West Azerbaijan province is Semi-arid, and is characterized by hot and dry summers, and wet and cold winters. This area possesses important wetlands such as Yadegarlou, Dashdurgah, Shourgol, Hassanlou, Agh Ghale, Seiran Goli and Sulduz Goli where hosts thousands of migrating birds. They play a key role in moderation of climate and ecosystem of this region. Further, Yadegarlou, Shourgol and Dashdurgah are among registered wetlands in the Ramsar convention on wetlands. Inasmuch as Sulduz wetlands located in the south of Lake Urmia, Area shrinkage or drying of these places can deteriorate the vulnerability of groundwater resources to infiltration of salty water that makes worse drought impacts consequently. The dominant land use, land cover types in the region include agricultural lands, residential areas, grasslands, wetlands and conservation lands.

2.2. Data and Processing

Suitable spatial and temporal resolutions of Landsat imagery and free access to them are reasons behind the selection of this satellite to study the mentioned wetlands of this region. Red, infrared and thermal bands related to 21 time series of the satellite (Path/Row: 168/34 & 169/34) were used in this study

(Table / Tablo 1) (Figure / Şekil 2). PC Spectral Sharpening algorithm (Welch and Ehlers, 1987) was used to sharpen the low resolution multi-band TM[®] images using 15 meter panchromatic band.

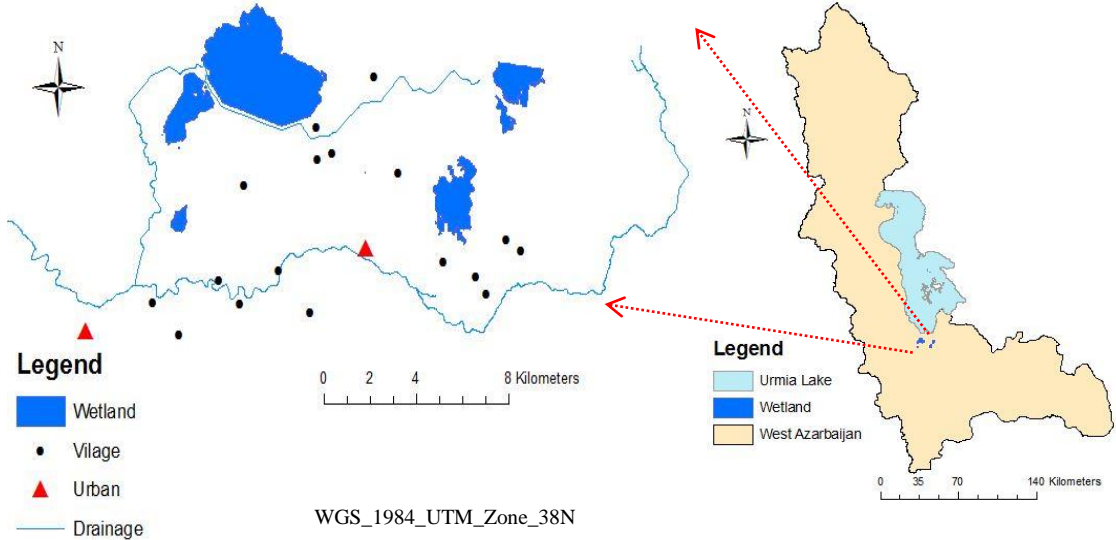


Figure 1. Study area (Sulduz region, Naghadeh city)
Şekil 1. Araştırma alanı (Sulduz bölgesi, Naghadeh şehri)

Table 1. Landsat 8 specification
Tablo 1. Landsat 8 özellikleri

1) Landsat-8 OLI and TIRS		
2) Bands	Wavelength (µm)	Resolution (m)
Band 1—Coastal aerosol	0.43–0.45	30
Band 2—Blue	0.45–0.51	30
Band 3—Green	0.53–0.59	30
Band 4—Red	0.64–0.67	30
Band 5—Near infrared (NIR)	0.85–0.88	30
Band 6—Short-wave infrared (SWIR 1)	1.57–1.65	30
Band 7—Short-wave infrared (SWIR 2)	2.11–2.29	30
Band 8—Panchromatic	0.50–0.68	15
Band 9—Cirrus	1.36–1.38	30
Band 10—Thermal infrared (TIRS) 1	10.60–11.19	100
Band 11—Thermal infrared (TIRS) 2	11.50–12.51	100

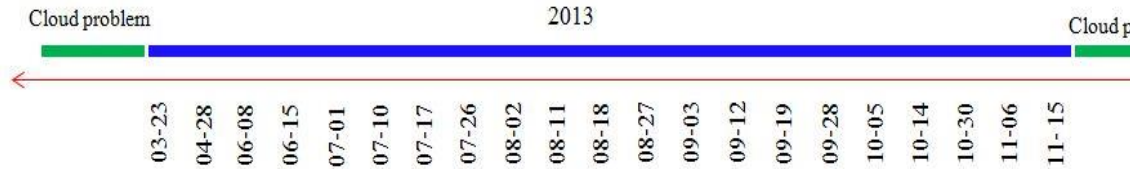


Figure 2. Landsat 8 time series (07:40 GMT)
Şekil 2. Landsat 8 zaman serileri (07:40 GMT)

The Landsat of 23 March 2013 is geo-referenced, using the nearest neighbor resampling method along with second degree polynomial equation and a 1/25000 topographic map of the area. Further, the other multitemporal Landsat 8 of 2013 is co-registered for 23 March 2013 imagery. The root mean squared error (RMSE) of less than 0.49 pixels (≈ 7 meters) has been attained.

The radiometric conversion of digital numbers (DN) to physical variables such as temperature requires radiometric calibration (Wukelic et al., 1989) and atmospheric correction (Cooper and Asrar 1989). DN values were converted to at-sensor radiance using the gain and bias coefficients of the detectors (Lamaro et al., 2013):

$$L_{\lambda} = gain * DN + bias \quad (1)$$

Where L_{λ} is the uncorrected spectral radiance at λ wavelength, DN the digital number, and gain and bias the calibration parameters of detectors. Gains and Biases of Landsat 8 thermal bands are as:

Gain (Band10&11) = Band-specific multiplicative rescaling factor = 3.3420E-04

Bias (Band10&11) = Band-specific additive rescaling factor = 0.10000

The equation used for atmospheric correction was (Srivastava et al., 2009):

$$L_{\lambda(T_s)} = \frac{L_{\lambda} - L_{\lambda up}}{t * \epsilon_{\lambda}} - \frac{1 - \epsilon_{\lambda}}{\epsilon_{\lambda}} * L_{\lambda down} \quad (2)$$

In this equation, $L_{\lambda(T_s)}$ is the corrected land surface radiance, L_{λ} is the uncorrected spectral radiance calculated in Eq. (1), $L_{\lambda up}$ is the upwelling radiance, t is the atmospheric transmissivity, ϵ_{λ} is the water emissivity, $L_{\lambda down}$ is the downwelling radiance. $L_{\lambda down}$, $L_{\lambda up}$ and t are atmospheric parameters which were obtained from Atmospheric Correction Parameter Calculator (<http://www.atmcorr.gsfc.nasa.gov>). That uses MODTRAN simulator (Barsi et al., 2003). NDVI threshold method was applied to determine the surface emissivity (ϵ_{λ}) and this parameter was divided into three categories according to NDVI values (Sobrino et al., 2004) :

- 3) $NDVI < 0.2$: indicates bare soil, and emissivity of bare soil is regarded as: $\epsilon_{soil} = .97$
- 4) $NDVI > 0.5$: represents areas with dense vegetation cover, and emissivity of vegetation cover is assumed as: $\epsilon_{veg} = .99$
- 5) $0.2 \leq NDVI \leq 0.5$: the pixels in this case are mixture of soil and vegetation cover. Emissivity (ϵ_{mix}) is calculated according to the following equation:

$$\epsilon = \epsilon_{veg} * P_v + \epsilon_{soil} * (1 - P_v) \quad (3)$$

Where P_v is proportion of vegetation cover and is computed as:

$$P_v = \left(\frac{NDVI - NDVI_{min}}{NDVI_{max} - NDVI_{min}} \right)^2 \quad (4)$$

In this equation, $NDVI_{min} = 0.2$ and $NDVI_{max} = 0.5$

Normalized differential Vegetation Index (NDVI) is one of the most popular methods for monitoring vegetation cover (Binh et al., 2005).

$$NDVI = \left(\frac{TM_5 - TM_4}{TM_5 + TM_4} \right) \quad (5)$$

Corrected surface radiance ($L_{\lambda(T_s)}$) were converted into surface temperature using Eq.6

$$T_s = \frac{K_2}{\ln \left(\frac{K_1}{L_{\lambda(T_s)} + 1} \right)} \quad (6)$$

Where T_s is surface temperature, K_1 calibration constant, (band 10, 11 = 774.89, 480.89), $L_{\lambda(T_s)}$ the corrected surface radiance and K_2 is another calibration constant (band10, 11 =1321.08, 1201.14) respectively. Both of the thermal bands of Landsat 8 (band 10&11) images were used to compute surface temperature which was calculated for these bands individually and then, the average was assessed accordingly.

3. RESULTS AND DISCUSSION

In this study, the spatial and temporal distribution of Sulduz wetlands was investigated using Landsat 8 imagery. Figure 3 illustrates the WST in the course of the study.

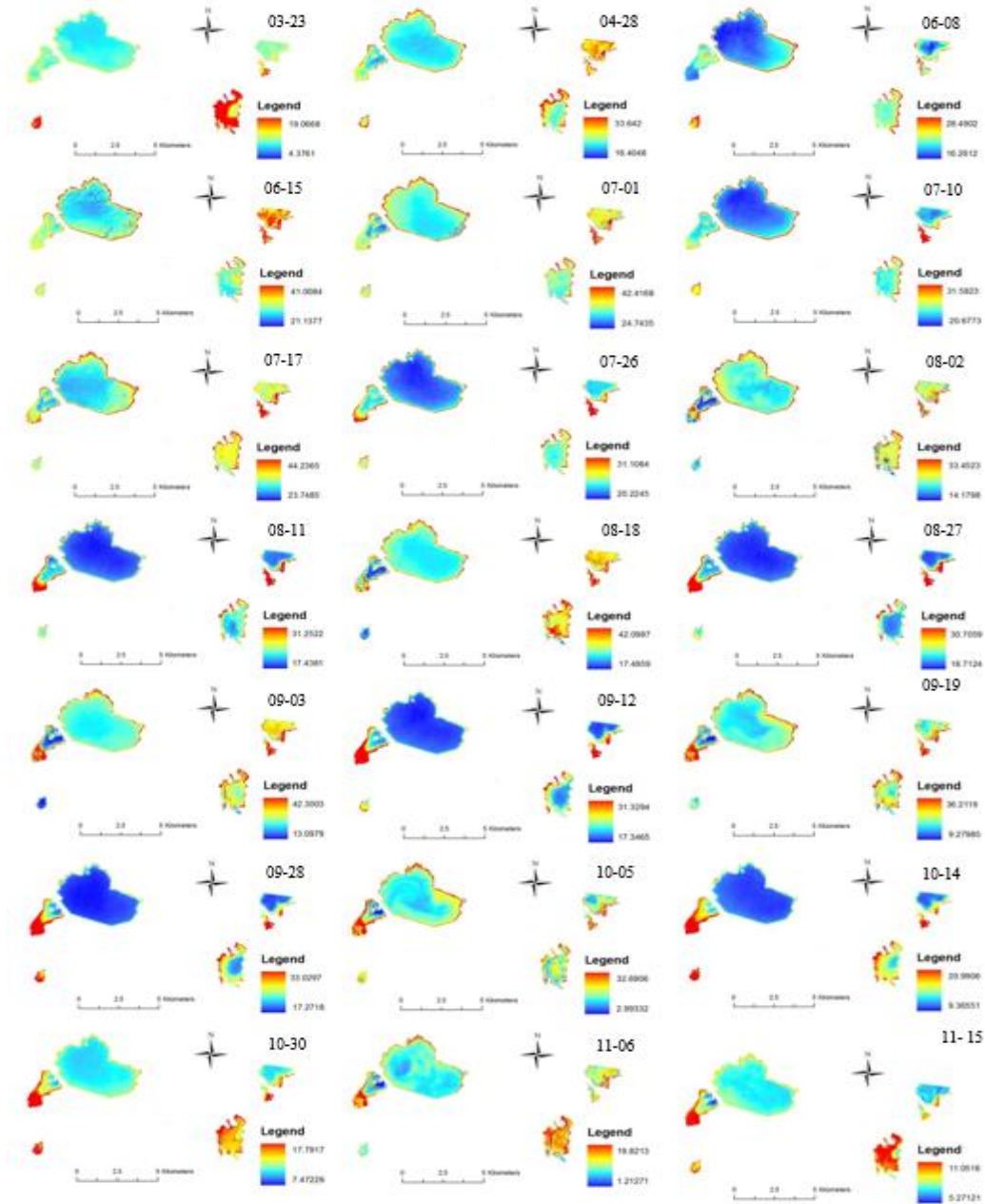


Figure 3. Spatial and temporal distributions of wetlands surface temperature ($^{\circ}\text{C}$) in 2013
 Şekil 3. 2013 yılında sulak alanların yüzey sıcaklığının ($^{\circ}\text{C}$) mekansal ve zamansal dağılımı

According to Figure / Şekil 3, WST experienced great spatial and temporal changes. The histogram distribution of surface temperature is shown in Figure / Şekil 4.

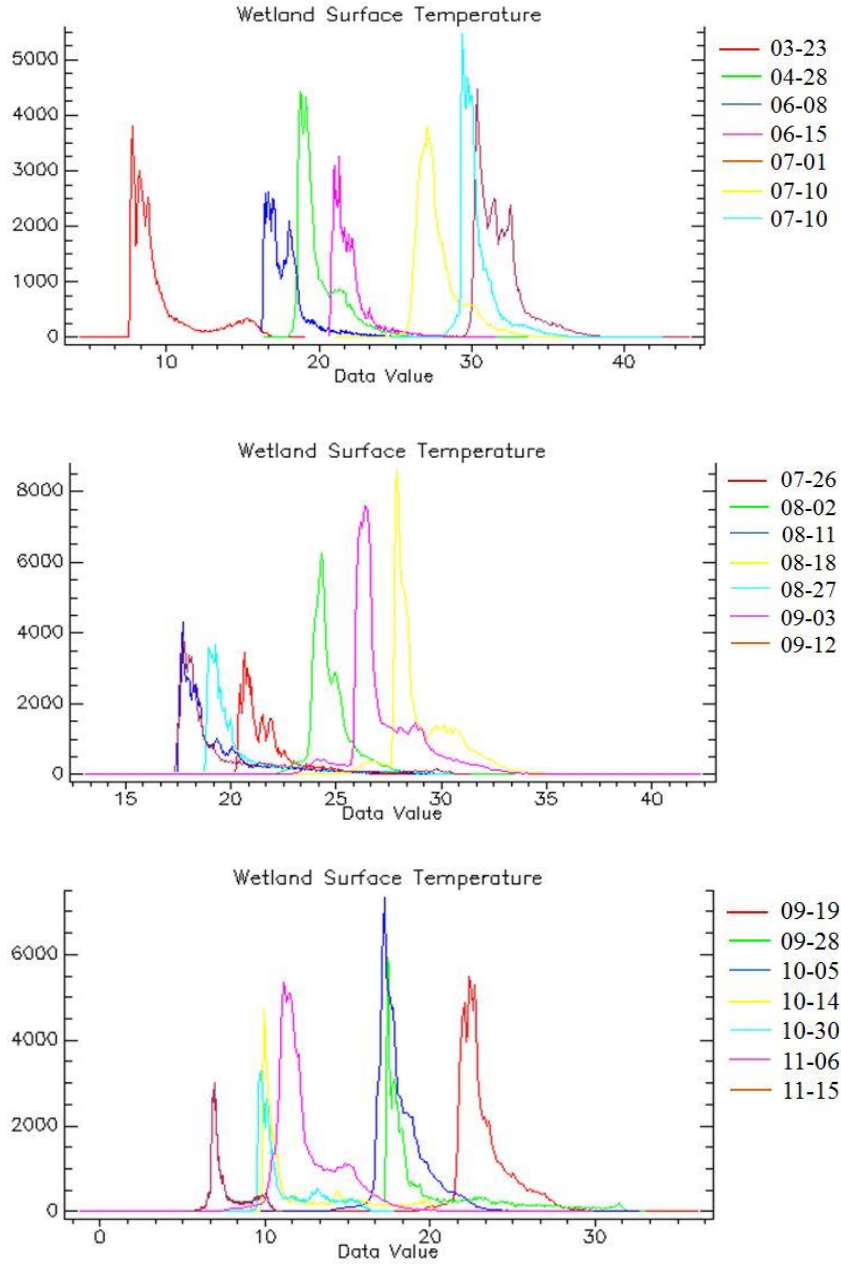


Figure 4. The histogram distribution of the WST in 2013
Şekil 4. 2013 yılında sulak alanların yüzey sıcaklıklarının (WST) histogram dağılımı

In this study, 21 different times of Landsat 8 imagery of 2013 were used. Figure / Şekil 5 depicts the average, the maximum, and the minimum values of the WST for each time.

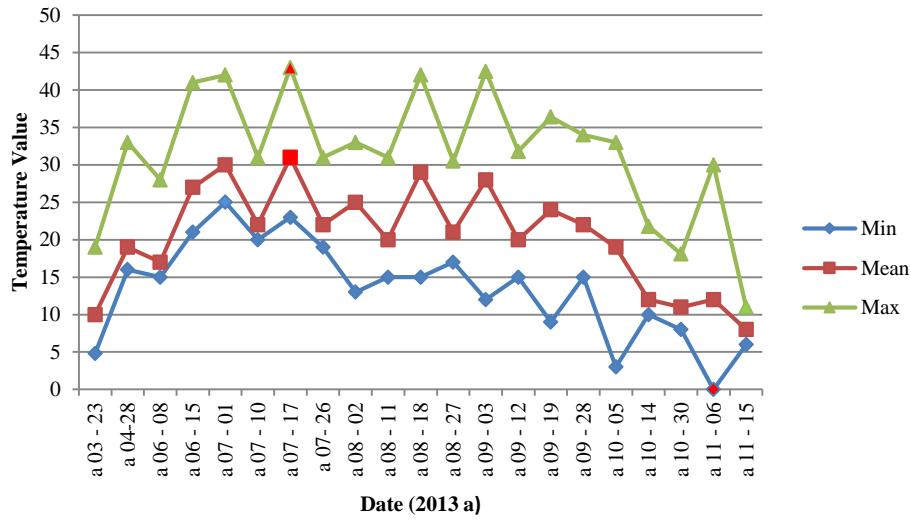


Figure 5. The minimum, maximum and average values of the WST by time

Şekil 5. Sulak alanların yüzey sıcaklıklarının (WST) zamana göre minimum, maksimum ve ortalama değerleri

The maximum value of the monthly temperature of Suldüz region is in July and Figure 5 confirms this term partly. Accordingly, WST of July (10.07.2013) has the highest value in both of maximum and average values. These results indicate that the WST is substantially affected by the air temperature. Meanwhile, the minimum value of WST corresponds to the November (06.11.2013). Spatial variations of the WST may be affected by numerous factors such as air temperature, entering the water flow to wetlands, entrance of industrial or agricultural pollutants, overgrowth of plants and biological activities. The standard deviation of spatial variations of wetlands temperature in the course of this study is illustrated in Figure 6.

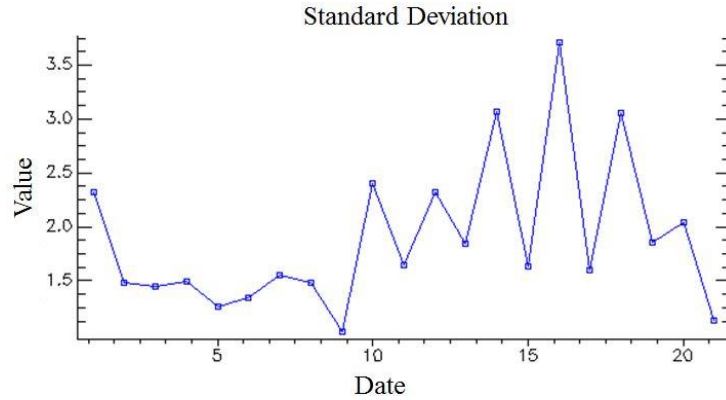


Figure 6. The standard deviation of the WST in the course of this study

Şekil 6. Sulak alanların yüzey sıcaklıklarının (WST) bu çalışma sırasındaki standart sapma değerleri

It shows August (02.08.2013) has the lowest spatial deviation of WST, which means the difference between the maximum and minimum range of temperature in August is low, and also high homogeneity prevails over the WST. On the other hand, June (28.06.2013) has the highest standard deviation that indicates heterogeneity, scattering and high thermal differences at this time. The overall average of the WST in Suldüz region is depicted in Figure / Şekil 7.

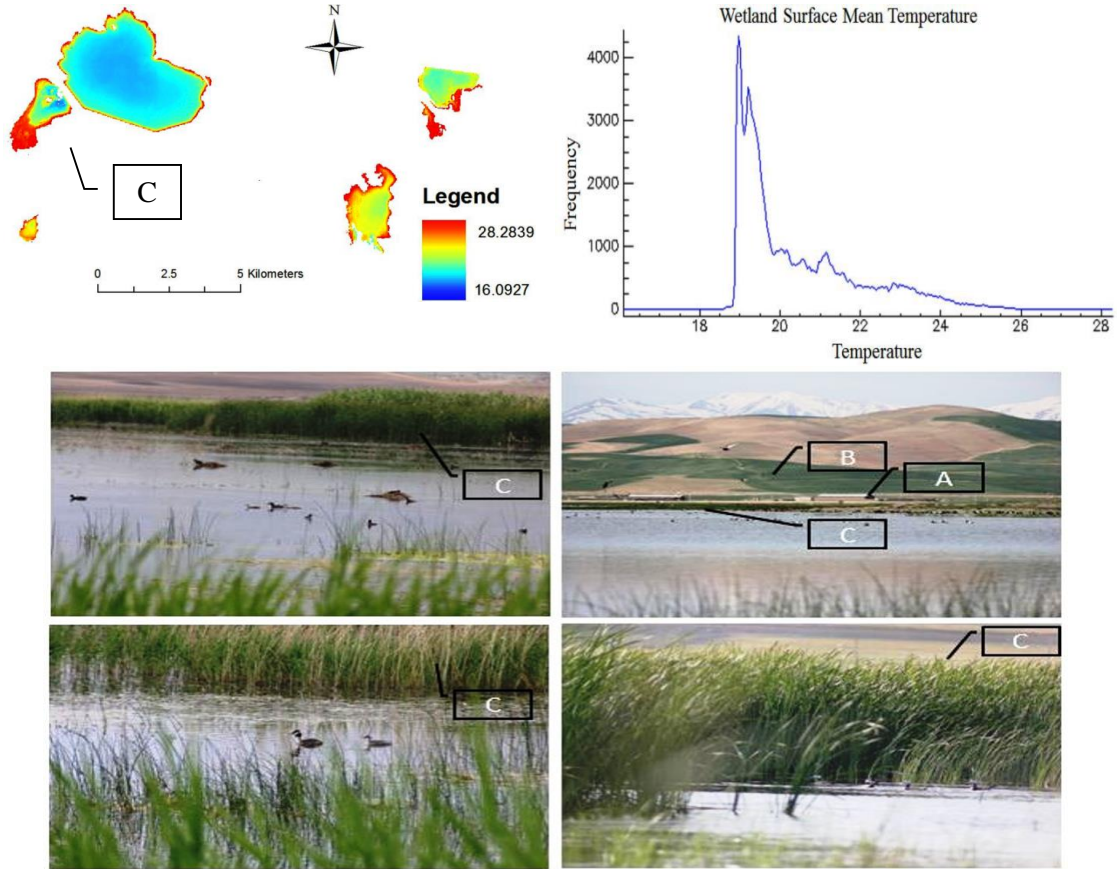


Figure 7. The average and histogram of the WST (°C) in 2013.

A: residential and industrial regions, **B:** agricultural lands, **C:** aquatic plants

Şekil 7. 2013 yılında sulak alanların yüzey sıcaklıklarının (WST) (°C) ortalama ve histogram dağılımı

A: ikamet ve endüstri bölgeleri, **B:** tarım alanları, **C:** su bitkileri

Figure / Şekil 7 shows that agricultural lands, industrial and residential areas located in the adjacent and the upstream part of wetlands can affect this ecosystem. The overgrowth of the aquatic plants can be seen in this figure. The shores and banks adjacent to industrial regions have higher surface temperatures than the central ones.

During the time, fluctuations and variations of WST have local differences. Figure / Şekil 7 depicts the temporal variance of these differences. It is apparent that those areas in the wetlands where they have higher variance experienced more severe temperature variations (Figure / Şekil 8). On the contrary, the low variance indicates stability and high thermal inertia throughout the time.

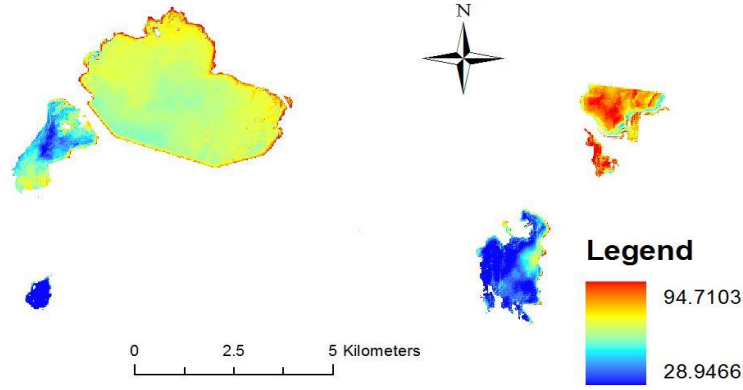


Figure 8. The temporal variance and the corresponding local differences of the WST in 2013. High values (red colure) show high temporal variance and vice versa low values (blue colure) is the regions with high thermal inertia
Şekil 8. 2013 yılında WST'ye karşılık gelen yerel ve zamansal değişiklikler. Yüksek değerler (kırmızı renk) yüksek zamansal değişimi ve düşük değerler (mavi renk) yüksek ısıl durgunluk olduğunu göstermektedir.

Due to entering agricultural and industrial pollutants in wetland ecosystem and also variations of water and air temperature, Wetlands vegetation covers fluctuate over time. In this study, NDVI was used to analyze the variation of vegetation cover. The NDVI value fluctuations have been displayed in Figure / Şekil 9.

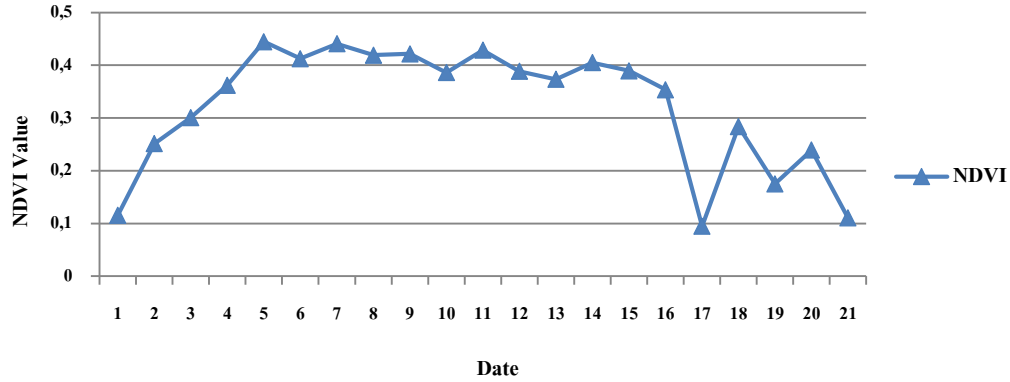


Figure 9. Wetlands NDVI variations in 2013
Şekil 9. 2013 yılında sulak alanların NDVI değişimleri

Correlation analysis was employed to assess the relationship between variations of vegetation cover and the WST changes. The resulting correlation coefficient between temporal changes of vegetation cover and the WST was found equal to 0.8. A scatter plot can suggest various kinds of correlations between variables. The relationship between the first component of NDVI time series (namely PC1) and the first component of the WST time series (namely PC1) is illustrated in Fig.10. By increasing of the vegetation cover area, the WST increased. However, the decrease of NDVI value and enlarging water coverage resulted in low WST. With regard to the relationship between these parameters, wetlands are categorized into 3 classes: 1) deep water, 2) shallow water with sparse vegetation cover and 3) shallow water with dense vegetation cover. Because of extensive water area, the concentration of scatter plot point in the first class is higher than the other classes.

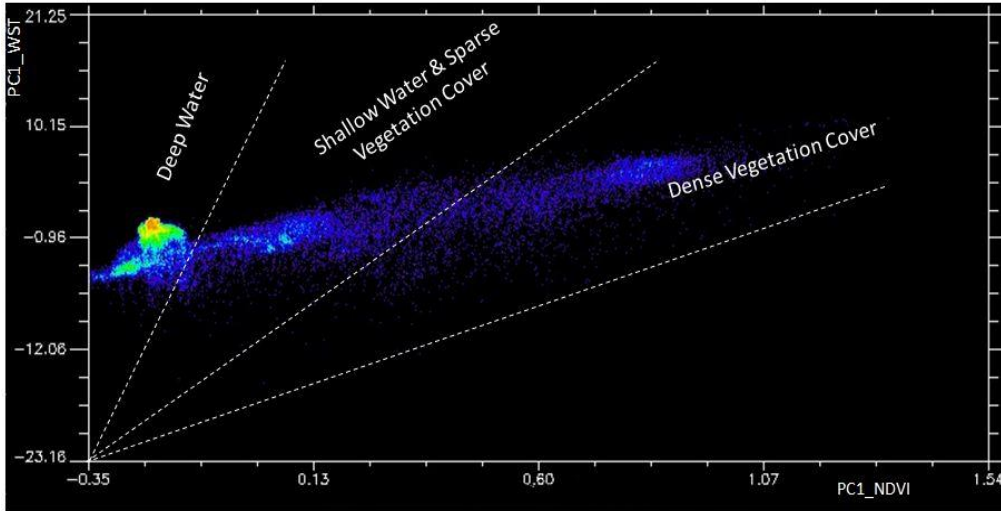


Figure 10. The scatterplot corresponding to first component of NDVI and the first component of WST
Şekil 10. NDVI ve WST ilk bileşenine karşılık gelen saçılım grafikleri

Our findings show that the WST has different spatial and temporal distribution. Wetlands banks have higher WST values due to low depth, dense vegetation cover, more soil coverage and adjacency to residential, industrial and agricultural zones. Since water has a higher specific heat and thermal inertia than soil and vegetation, these properties leads to later warming of water in comparison to soil and vegetation cover during daytime. Matzinger et al., (2007) stated that oxygen concentration in water is sensitive to the temperature and global warming. Accordingly, the map related to spatial distribution of the WST is useful for illustrating the distribution of soluble oxygen concentration in water. Therefore, these maps can be beneficial for the management and monitoring health of the aquatic creatures. Temperature and moisture regimes are among the key variables that determine the distribution, growth and productivity, and reproduction of plants and animals. Changes in hydrology can influence species in a variety of ways, but the most completely understood processes are those that link moisture availability with intrinsic thresholds that govern metabolic and reproductive processes (Burkett et al., 2005). Temperature can exert its influence on species through changes in moisture availability. The high variability of water temperature can lead to many harmful effects on the aquatic creatures and the birds in the wetlands. On the other hand, regions with low thermal fluctuations indicate ecosystem health and stability. By taking into consideration that the study region covers a small area, its climate can be assumed homogenous. Therefore, spatial differences in the WST cannot contribute to different climatic conditions. This phenomenon is usually occurs as a result of influx of different pollutants into these areas which leads to increase of the spatial standard deviation of the WST. The resulting map from the temporal variance of WST can reveal thermal stable and unstable zones where the unstable ones can take priority for field investigation in terms of the influx of pollutant materials into wetlands, and ecosystem degradation susceptibility mapping.

The study findings show that evaporation, water area shrinkage and increase of lands coverage along the wetlands banks result in rise of temperature in these regions. If these adverse conditions persist, the rise of the ground surface temperature will also have an incremental trend. These results confirm the key role of wetlands in moderating of the ground and air temperature. Further, consideration of the correlation analysis suggests a meaningful relationship between thermal variations and the vegetation cover.

Wetlands of Sulduz region is located downstream of agricultural lands where Entrance of the agricultural sediments and pollutants leads to decrease of their depth on the one hand and intensifies the overgrowth of aquatic plants on the other hand. Thus, agricultural activities affect the WST fluctuations indirectly. Accordingly, the outcome demonstrates that land use land cover effectively contribute to wetland ecosystem health. The study findings are useful for the water management, prevention from drying of these locations and evapotranspiration modeling.

The approach employed in this research indicates that remote sensing is a valuable, low-cost and stable tool for thermal monitoring of wetlands health. However, more extensive application was limited by the cloud cover problem which resulted in a decrease of the temporal coverage related to cold months of the year. To overcome this problem, use of other sensors imagery such as AVHRR and MODIS along with Landsat 8 imagery is recommended.

REFERENCES (KAYNAKLAR)

- Ahn, Y., Shanmugam, P., Lee, J., Kang, Y., 2006. Application of satellite infrared data for mapping of thermal plume contamination in coastal ecosystem of Korea. *Marine Environmental Research* 61: 186–201, doi: <http://dx.doi.org/10.1016/j.marenvres.2005.09.001>
- Alcantara, E., Barbosa, C., Stech, J., Novo, E., Shimabukuro, Y., 2009. Improving the spectral unmixing algorithm to map water turbidity distributions. *Environmental Modelling and Software* 24: 1051–1061, doi: <http://dx.doi.org/10.1016/j.envsoft.2009.02.013>
- Alcantara, E.S., Tech, J., Lorenzetti, J., Bonnet, M.P., Casamitjana, X., Assireu, A.T., Novo, E., 2010. Remote sensing of water surface temperature and heat flux over a tropical hydroelectric reservoir. *Remote Sensing of Environment* 114: 2651–2665.
- Barsi, J.A., Barker, J.L., Schott, J.R., 2003. An Atmospheric Correction Parameter Calculator for a Single Thermal Band Earth-Sensing Instrument. Paper presented at the IGARSS03, Toulouse, France, doi: <http://dx.doi.org/10.1109/IGARSS.2003.1294665>
- Beauchamp, E.G., Trevors, J.T., Paul, J.W., 1989. Carbon sources for bacterial denitrification. *Advance in Soil Science* 10:113–142.
- Bergstedt, R., Argyle, R.L., Seelye, J.G., Scribner, K.T., Curtis, G.L., 2003. In situ determination of the annual thermal habitat use by Lake Trout (*Salvinus namaycush*) in Lake Huron. *Journal of Great Lakes Research* 29: 347–361.
- Binh, T.N.K.D., Vromant, N., Hung, N.T., Hens, L., Boon, E.K., 2005. Landcover changes between 1968 and 2003 in CaiNuoc, Ca Mau Peninsula, Vietnam *Environment, Development and Sustainability* 7: 519–536.
- Bremner, J.M., Shaw, K., 1958. Denitrification in soil. II. Factors affecting denitrification. *Journal of Agricultural Science* 51: 40–52.
- Burkett, V.R., Wilcox, D.A., Stottlemeyer, R., Barrow, W., Fagre, D., Baron, J., Price, J., Nielsen, J.L., Allen, C.D., Peterson, D.L., Ruggerone, G., Doyle, T., 2005. Nonlinear dynamics in ecosystem response to climate change: Case studies and policy implications. *Ecological Complexity* 2: 357–394, doi: <http://dx.doi.org/10.1016/j.ecocom.2005.04.010>
- Bussi eres, N., Granger, R.J., 2007. Estimation of Water Temperature of Large Lakes in Cold Climate Regions during the Period of Strong Coupling between Water and Air Temperature Fluctuations. *Journal of Atmospheric and Oceanic Technology* 24: 285–296.
- Chavula, G., Brezonik, P., Thenkabail, P., Johnson, T., Bauer, M., 2009. Estimating the surface temperature of Lake Malawi using AVHRR and MODIS satellite imagery. *Physics and Chemistry of the Earth* 34: 749–754, doi: <http://dx.doi.org/10.1016/j.pce.2009.08.001>
- Cherkauer, K. A., Burges, S.J., Handcock, R.N., Kay, J.E., Kampf, S.K., Gillespie, A.R., 2005. Assessing satellite-based and aircraft-based thermal infrared remote sensing for monitoring Pacific Northwest River temperature. *Journal of the American Water Resources Association* 41: 1149–1159.
- Coats, R., 2010. Climate change in the Tahoe basin: regional trends, impacts and drivers. *Climate Change* 102: 435–466, doi: <http://dx.doi.org/10.1007/s10584-010-9828-3>
- Cooke, S.J., Bunt, C.M., Schreer, J.F., 2004. Understanding fish behavior, distribution, and survival in thermal effluents using fixed telemetry arrays: a case study of smallmouth bass in a discharge canal during winter. *Environmental Management* 33: 140–150.

- Cooper, D.I., Asrar, G., 1989. Evaluating atmospheric correction models for retrieving surface temperatures from the AVHRR over a tall grass prairie. *Remote Sensing of Environment Supports* 27: 93–102.
- Dash, P., Gottsche, F.M., Olesen, F.S., Fischer, H., 2002. Land surface temperature and emissivity estimation from passive sensor data: theory and practice-current trends. *International Journal Remote Sensing* 23:2563–2594, doi: <http://dx.doi.org/10.1080/01431160110115041>
- Fiedler, E., Martin, M., Roberts-Jones, J., 2012. Lake Surface Water Temperature in the operational OSTIA system. Met Office Forecasting Research Technical Report no. 565.
- Gibbons, D.E., Wukelic, G.E., 1989. Application of Landsat thematic mapper data for coastal thermal plume analysis at Diablo Canyon. *Photogrammetric Engineering and Remote Sensing* 55: 903–909.
- Gillet, C., Péquin, P., 2006. Effect of temperature changes on the reproductive cycle of roach in Lake Geneva from 1983 to 2001. *Journal of Fish Biology* 69: 518–534, doi: <http://dx.doi.org/10.1111/j.1095-8649.2006.01123.x>
- Gilman, K., 1994. Hydrology and wetland conservation. Chichester. Wiley.
- Gleason, R.A., Euliss, N.H., Hubbard, D.E., Duffy, W.G., 2003. Effect of sediment load on the emergence of aquatic invertebrates and plants from wetland soil egg and seed banks. *Wetlands* 23: 26–34, doi: [http://dx.doi.org/10.1672/0277-5212\(2003\)023%5B0026:EOSLOE%5D2.0.CO;2](http://dx.doi.org/10.1672/0277-5212(2003)023%5B0026:EOSLOE%5D2.0.CO;2)
- Ham, J., Toran, L., Cruz, J., 2006. Effect of upstream ponds on stream temperature. *Environmental Geology* 50: 55–61, doi: <http://dx.doi.org/10.1007/s00254-006-0186-4>
- Harding, J.S., Young, R.G., Hayes, J.W., Shearer, K.A., Stark, J.D., 1999. Changes in agricultural intensity and river health along a river continuum. *Freshwater Biology Journal* 42: 345–357, doi: <http://dx.doi.org/10.1046/j.1365-2427.1999.444470.x>
- Jeppesen, E., Mehner, T., Winfield, J., 2012. Impacts of climate warming on the long-term dynamics of key fish species in 24 European lakes. *Hydrobiologia* 694:1–39, doi: <http://dx.doi.org/10.1007/s10750-012-1182-1>
- Klotz, R.L., 1985. Factors controlling phosphorus limitation in stream sediments. *Limnology and Oceanography* 30: 543–553, doi: <http://dx.doi.org/10.4319/lo.1985.30.3.0543>
- Lamaro, A.A., Marinelarena, A., Torrusio, S., Sala, S., 2013. Water surface temperature estimation from Landsat7 ETM+ thermal infrared data using the generalized single-channel method: Case study of Embalse del RíoTercero (Cordoba, Argentina). *Advances in Space Research* 51: 492–500.
- Matzinger, A., Schmid, M., Veljanoska-Sarafiloska, E., Patceva, S., Guseska, D., Wagner, B., Müller, B., Sturm, M., Wüest, A., 2007. Eutrophication of ancient Lake Ohrid: global warming amplifies detrimental effects of increased nutrient inputs. *Limnology and Oceanography* 52: 338–353, doi: <http://dx.doi.org/10.4319/lo.2007.52.1.0338>
- Mortsch, L.D., Quinn, F.H., 1996. Climate change scenarios for Great Lake basin ecosystem studies. *Limnology and Oceanography* 41: 903–911, doi: <http://dx.doi.org/10.4319/lo.1996.41.5.0903>
- Nehorai, R., Lensky, I.M., Lensky, N.G., Shiff, S., 2009. Remote sensing of the Dead Sea surface temperature. *Journal of Geophysical Research* 114: 4-11, doi: <http://dx.doi.org/10.1029/2008JC005196>
- Novo, E.L., Barbosa, C.C.F., Freitas, R.M., Shimabukuro, Y.E., Melack, J.M., Pereira-Filho, W., 2006. Seasonal changes in chlorophyll distribution in Amazon flood plain lakes derived from MODIS images. *Limnology* 7: 153–161.
- Paerl, H.W., Paul, V.J., 2012. Climate change: links to global expansion of harmful cyanobacteria. *Water Research* 46: 1349–1363, doi: <http://dx.doi.org/10.1016/j.watres.2011.08.002>
- Piao, D.X., Wang, F.K., 2011. Environmental conditions and the protection counter-measures for waters of Lake Xingkai. *Lake Science* 23:196–202.
- Reinart, A., Reinhold, M., 2008. Mapping surface temperature in large lakes with MODIS data. *Remote Sensing of Environment* 112: 603–611, doi: <http://dx.doi.org/10.1016/j.rse.2007.05.015>

- Relyea, R.A., 2005. The impact of insecticides and herbicides on the biodiversity and productivity of aquatic communities. *Ecological Applications* 15: 618–627, doi: <http://dx.doi.org/10.1890/03-5342>
- Schneider, P., Hook, S.J., Radocinski, R.G., Corlett, G.K., Hulley, G.C., Schladow, S.G., Steissberg, T.E., 2009. Satellite observations indicate rapid warming trend for lakes in California and Nevada. *Geophysical Research Letters* 36: L22402, doi: <http://dx.doi.org/10.1029/2009GL040846>
- Sharpley, A.N., Withers, P.J., 1994. The environmentally-sound management of agricultural phosphorus. *Fertilizer Research* 39: 133–146, doi: <http://dx.doi.org/10.1007/BF00750912>
- Sobrino, J.A., Jiménez, M., Paolinib, C.J., 2004. surface temperature retrieval from LANDSAT TM 5. *Remote Sensing of Environment* 90: 434-440, doi: <http://dx.doi.org/10.1016/j.rse.2004.02.003>
- Srivastava, P.K., Majumdar, T.J., Bhattacharya, A.K., 2009. Surface temperature estimation in Singhbhum Shear Zone of India using Landsat-7 ETM+ thermal infrared data. *Advances in Space Research* 43: 1563–1574, doi: <http://dx.doi.org/10.1016/j.asr.2009.01.023>
- Strub, P.T., Powell, T.M., 1986. Wind-driven surface transport in stratified closed basins: Direct versus residual calculation. *Geophysical Journal International* 91:8497–8508.
- Steissberg, T.E., Hook, S.J., Schladow, S.G., 2005. Measuring surface currents in lakes with high spatial resolution thermal infrared imagery. *Geophysical Research Letters* 32: L11402, doi: <http://dx.doi.org/10.1029/2005GL022912>
- Steissberg, T.S., Hook, S., Schladow, S., 2005. Characterizing partial upwellings and surface circulation at Lake Tahoe, California–Nevada, USA with thermal infrared images. *Remote Sensing of Environment* 99:2-15, doi:<http://dx.doi.org/10.1016/j.rse.2005.06.011>
- Strub, P.T., Powell, T.M., 1987. Surface temperature and transport in Lake Tahoe: Inferences from satellite (AVHRR) imagery. *Continental Shelf Research* 7:1001–1013, doi: [http://dx.doi.org/10.1016/0278-4343\(87\)90096-3](http://dx.doi.org/10.1016/0278-4343(87)90096-3)
- Wan, Z., 2008. New refinements and validation of the MODIS Land-Surface Temperature/Emissivity products. *Remote Sensing of Environment* 112: 59-74, doi: <http://dx.doi.org/10.1016/j.rse.2006.06.026>
- Welch, R., Ehlers, W., 1987. Merging Multi resolution SPOT HRV and Landsat TM Data. *Photogrammetric Engineering and Remote Sensing* 53: 301-303.
- Wooster, M., Patterson, G., Loftie, R., Sear, C., 2001. Derivation and validation of the seasonal thermal structure of Lake Malawi using multi-satellite AVHRR observations. *International Journal of Remote Sensing* 22: 2953–2972, doi: <http://dx.doi.org/10.1080/01431160010006999>
- Wukelic, G.E., Gibbons, D.E., Martucci, I.M., Foote, H.P., 1989. Radiometric calibration of Landsat thematic mapper thermal band. *Remote Sensing of Environment* 28: 339–347, doi: [http://dx.doi.org/10.1016/0034-4257\(89\)90125-9](http://dx.doi.org/10.1016/0034-4257(89)90125-9)
- Zoran, M.A., Nicola, D.N., Talianu, C.L., Ciobanu, M., Ciuciu, J.G., 2005. Analyses of thermal plume of Cernavoda nuclear power plant by satellite remote sensing data, in: Manfred Ehlers, Ulrich Michel (Eds.). *Proceedings of the Remote Sensing for Environmental Monitoring, GIS Applications, and Geology V*.